Engineering Structures 130 (2017) 99–111

Contents lists available at ScienceDirect

Engineering Structures

journal homepage: www.elsevier.com/locate/engstruct

# Improving seismic performance of framed structures with steel curved dampers

H.-L. Hsu *, H. Halim

*Dept. of Civil Engineering, National Central University, Chung-Li 32054, Taiwan*

ARTICLE INFO

*Article history:*
Received 20 June 2016
Revised 25 September 2016
Accepted 29 September 2016

*Keywords:*
Semi-rigid frames
Steel curved dampers
Energy dissipation
Seismic performance

ABSTRACT

Moment resisting frames possess significant ductility and thus are commonly used in earthquake-resistant designs. However, excessive deformation due to lower stiffness and structural strength limits the applicability of this system. Steel curved dampers are proposed in this study to improve this system's structural performance. The curved dampers were laser-cut from steel plates with the desired geometries and placed at the beam to column regions. The damper behavior is governed by its length and angle between the two ends. A series of cyclic loading tests were performed on steel frames with various curved damper placements to evaluate the curved damper effect on the structural performance. It was found from the test results that the frame strength was higher when the damper angle was smaller. It was also observed from test result comparisons that significant improvements in strength, stiffness and energy dissipation were achieved when the proposed curved dampers were added to the moment resisting frames. Information obtained from this preliminary investigation will be used as data for comparisons in further study of dynamic behavior of multi-story framed structures.

## 1. Introduction

Steel rigid frames and semi-rigid frames are commonly used for construction in areas with seismic activities [1–8]. Rigid frames possess high strength to resist lateral force induced by earthquakes. However, rigid frame design concerns have been raised due to a number of failures related to the fractures of welded beam-to-column connections under major earthquakes. Heavy stress concentration in the welds causing premature brittle failure in the connections leads to major strength deterioration and performance loss [9–15].

Semi-rigid frames are usually constructed using bolt connections between the beams and columns. This frame construction exhibits adequate deformation capability when subjected to cyclic loads. The semi-rigid higher deformation capability greatly reduces the brittle failure potential of the structures, however, excessive deformation due to lower structural stiffness and insufficient energy dissipation in the bolt connections remain concerns when adequate seismic performance is required [16–23]. Design modification in the beam-to-column regions that sustain structural strength and increase energy dissipation capability is essential [24–32].

This study focused on framed structure performance improvement by integrating semi-rigid frames with new steel curved dampers in the beam-to-column joint corner regions, as shown in Fig. 1. The proposed curved dampers were laser-cut from steel plates with the desired geometries. Curved dampers were hinged to the beams and columns to simplify the connection designs. The distance between the damper centroid and the load action axis was equivalent to a prescribed eccentricity. Therefore, the curved damper could be easily bent when an external load was applied to the structure, yielding to dissipate energy at early stage frame deformation, preventing major structural members from being damaged. A series of cyclic load tests were conducted on the steel frames with various curved damper placements. Test results obtained from this preliminary investigation, such as frame strength, stiffness and energy dissipation were compared to evaluate the proposed design method effectiveness and justify its feasibility in engineering practice.

## 2. Strength of curved dampers

The curved damper geometry is shown in Fig. 2. As indicated in this figure, an additional moment ($P\Delta$) due to the curved damper eccentricity will be incurred when the damper is subjected to an axial force, $P$. The eccentricity magnitude, $\Delta$, can be evaluated using the following expression:

---

* Corresponding author.
*E-mail address:* hhsu@ncu.edu.tw (H.-L. Hsu).

http://dx.doi.org/10.1016/j.engstruct.2016.09.063
0141-0296/

**Nomenclature**

| | | | |
|---|---|---|---|
| $P$ | axial force | $\sigma_{max}$ | maximum stress |
| $P_y$ | yielding strength of the damper | $\sigma_y$ | yielding stress of the material |
| $\varDelta$ | eccentricity | $d$ | depth of the damper |
| $R$ | radius of the curved damper | $t$ | thickness of the damper |
| $\theta$ | angle between the two ends of the damper | $I$ | moment of inertia of the curved damper |
| $L$ | damper length | | |

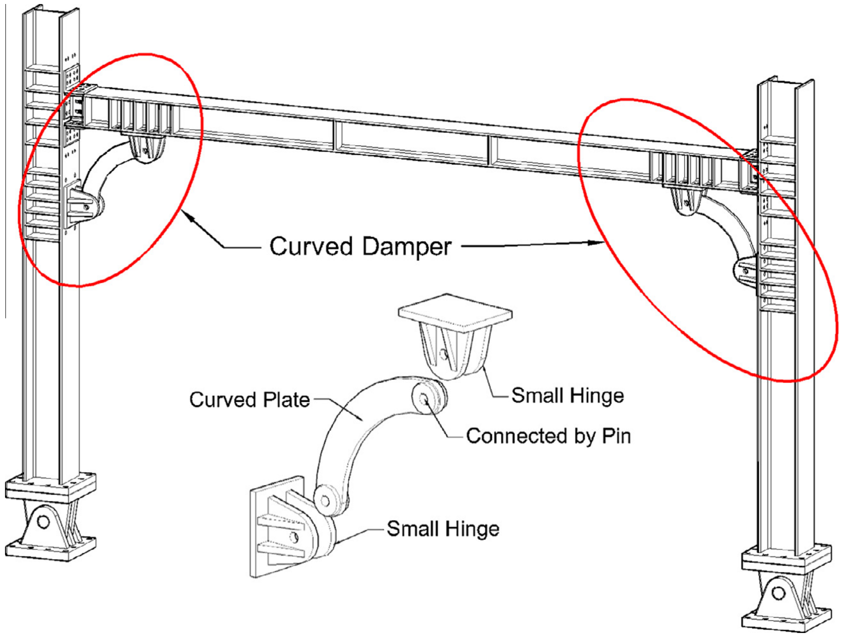

**Fig. 1.** Description of the design proposal.

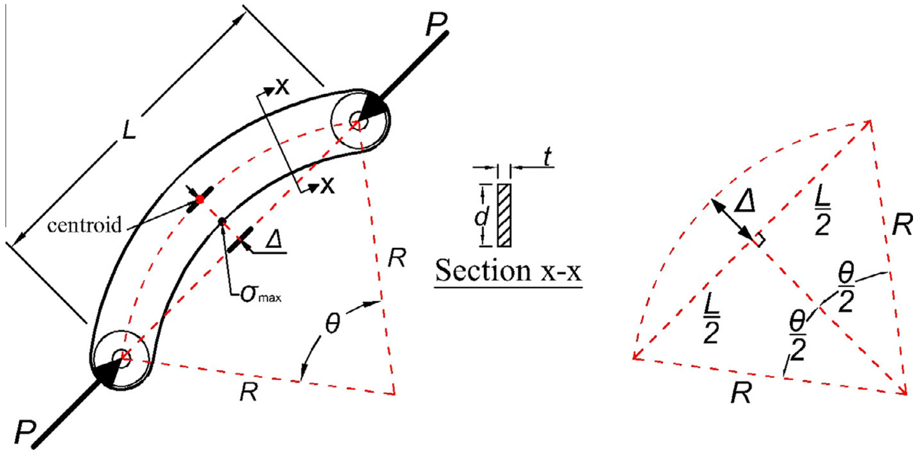

**Fig. 2.** Geometry of the curved damper.

$$\Delta = R - R\cos\frac{\theta}{2} \tag{1}$$

In which, $R$ is the radius of the curved damper and $\theta$ is the angle between the two damper ends, as defined in Fig. 2. The relationship among the damper length, $L$, damper angle, $\theta$, and damper radius, $R$, can be defined by the following:

$$\frac{L}{2} = R\sin\frac{\theta}{2} \tag{2}$$

Therefore, the curved damper eccentricity can be obtained using:

$$\Delta = \frac{L(1-\cos\frac{\theta}{2})}{2\sin\frac{\theta}{2}} \tag{3}$$

For curved damper subject to axial force $P$, the maximum stress ($\sigma_{max}$) on the curved damper is located at the inner-center of the curved damper and can be evaluated using the following expression:

$$\sigma_{max} = \frac{M\left(\frac{d}{2}\right)}{I} + \frac{P}{A} \tag{4}$$

or,

$$\sigma_{max} = \frac{P\Delta\left(\frac{d}{2}\right)}{\frac{1}{12}d^3t} + \frac{P}{dt} \tag{5}$$

In which, $d$ and $t$ are the damper depth and thickness, respectively.

The damper reaches yielding and effectively dissipates energy when the maximum stress is equal to the material yielding stress, $\sigma_y$. Therefore, the damper yielding strength, $P_y$, can be calculated using the following expression:

$$P_y = \frac{d^2t}{6\Delta + d}\sigma_y \tag{6}$$

The curved damper hysteretic behavior is described using the example shown in Fig. 3. In this example, a SN400YB damper with yielding stress equaling 293 MPa was subject to cyclic load. The damper thickness ($t$) and depth ($d$) were 20 mm and 100 mm, respectively. The damper length equaled 537 mm and the damper angle was 60°, which resulted in 72 mm of damper eccentricity. The figure shows that the curved damper exhibited stable hysteretic behavior and similar strength under tension and compression. This characteristic effectively alleviated the significant strength deterioration concern due to member buckling. The yielding strength of this damper evaluated according to Eq. (6) was 110 kN, which was validated using the result obtained from the numerical analysis using ANSYS [33], as shown in this figure.

## 3. Experimental program

### 3.1. Preliminary evaluation for frame responses

In order to define the relationship between frame response and damper placements for subsequent experimental verification, a series of analytical simulations on semi-rigid frames with various dampers were carried out using ANSYS. The parameters considered in the preliminary designs included the curved damper length and angle. Table 1 lists the frame details considered in the numerical simulation. These frames were subjected to push-over loads up to 5% drift ratio.

Fig. 4 describes the considered frame stress distributions. The figure shows that critical stress at the beam-to-column connections was effectively shifted to the prescribed curved dampers, as expected, which justified the design feasibility. The relationship between the frame strength, i.e. the capacity of the system, and the various damper geometries, i.e. length and angles, is shown in Fig. 5. The figure shows that frame strength decreases when the damper angle increases. Further comparison on the relationship between frame strength and curved damper eccentricities, as shown in Fig. 6, revealed that the frame strength was greatly influenced by the damper eccentricity magnitude. Therefore, it is essential that the damper geometries be adequately determined so that significant structural performance could be achieved.

### 3.2. Test specimens

Eight steel frames including one semi-rigid frame, one rigid frame and six semi-rigid frames with various curved dampers were fabricated for testing to validate the proposed system's effectiveness. The test frame height and span were 2520 mm and 4744 mm, respectively. Identical columns and beams, H250 × 250 × 9 × 14 and H200 × 200 × 8 × 12, respectively, were used for all test frames. This combination formed a strong column/weak beam mechanism with strength ratio equaling 1.88. For semi-rigid connections, L130 × 130 × 12 was used for the top and seat angles and L100 × 100 × 10 with slots were adopted in the double web angles. The web angles were used to provide connection shear strength and the slot was used to maintain structure safety should the top and seat angles be damaged during the loading process. For rigid frames, the beam was welded to a pair of 30-mm end plates and connected to the columns using high strength bolts. The beam, column, steel angle and curved dampers were all made of SN400YB steel with yield stress equaling 300 MPa, 300 MPa, 314 MPa and 293 MPa, respectively. A574 M high strength bolts were used for all connections. Fig. 7 shows the test frame details. Semi-rigid and rigid frame test results were used

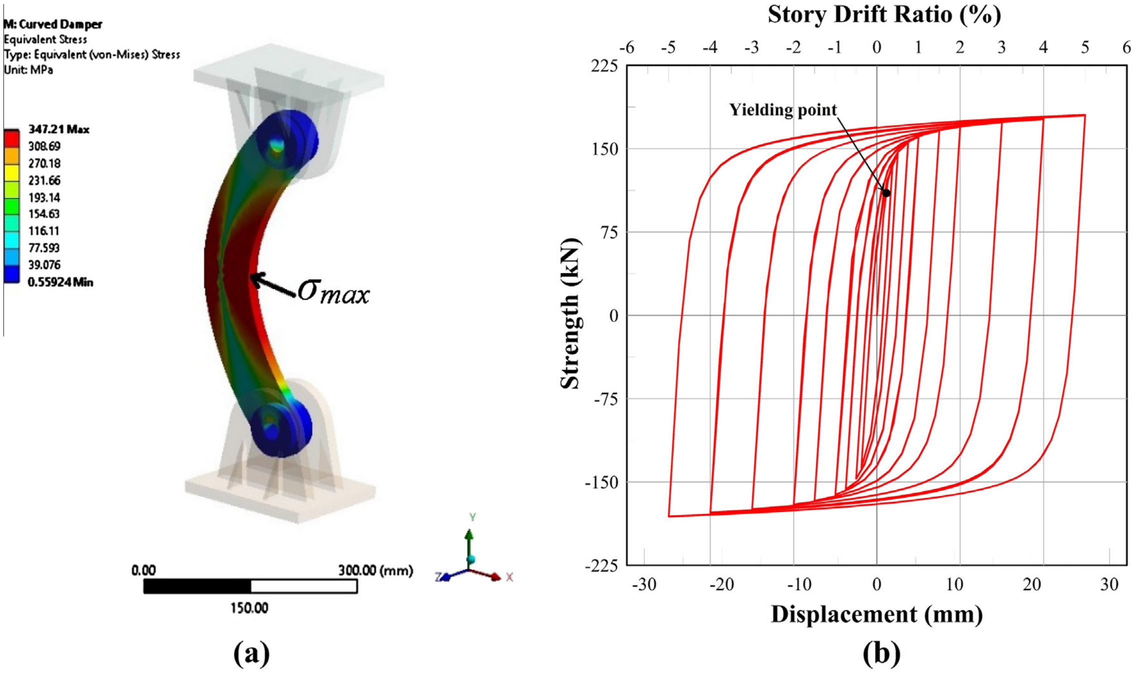

**Fig. 3.** Responses of curved damper subject to cyclic load. (a) Stress distribution; (b) hysteretic loops.

**Table 1**
Details of frames used for preliminary response evaluation.

| Test group | Damper angle (°) | Frame label | Damper length $L$ (mm) | Damper eccentricity $\Delta$ (mm) | Strength at 5% drift (kN) |
|---|---|---|---|---|---|
| L0 | 60 | L0-60 | 311 | 41.7 | 167.4 |
| | 75 | L0-75 | | 52.8 | 151 |
| | 90 | L0-90 | | 64.4 | 137.8 |
| | 120 | L0-120 | | 89.8 | 117.1 |
| L1 | 60 | L1-60 | 424 | 56.8 | 157.4 |
| | 75 | L1-75 | | 72.0 | 139.7 |
| | 90 | L1-90 | | 87.9 | 125.9 |
| | 120 | L1-120 | | 122.5 | 107.5 |
| L2 | 60 | L2-60 | 537 | 72.0 | 149.6 |
| | 75 | L2-75 | | 91.2 | 132 |
| | 90 | L2-90 | | 111.3 | 119.4 |
| | 120 | L2-120 | | 155.1 | 102 |
| L3 | 60 | L3-60 | 651 | 87.2 | 143.9 |
| | 75 | L3-75 | | 110.4 | 127.4 |
| | 90 | L3-90 | | 134.7 | 114.9 |
| | 120 | L3-120 | | 187.8 | 98.4 |
| L4 | 60 | L4-60 | 764 | 102.3 | 139.8 |
| | 75 | L4-75 | | 129.6 | 122.9 |
| | 90 | L4-90 | | 158.2 | 111.1 |
| | 120 | L4-120 | | 220.5 | 95.3 |
| L5 | 60 | L5-60 | 877 | 117.5 | 136.4 |
| | 75 | L5-75 | | 148.8 | 120.6 |
| | 90 | L5-90 | | 181.6 | 109.1 |
| | 120 | L5-120 | | 253.1 | 93.6 |

to set the data for comparison and evaluate the performance enhancement when the curved dampers were adopted in the frame designs.

Six dampers with various geometries were selected, based on the finite element simulation stated above, and installed into semi-rigid frames to identify the curved damper effect in improving framed structure performance. The curved dampers were laser-cut from 20-mm steel plates with desired geometries. These curved dampers varied in length ($L$) and angle ($\theta$) between the two device pin ends. The six dampers could be divided into three groups, L1, L2 and L3, with damper lengths equaling 424 mm, 537 mm, and 651 mm, respectively. A complete set of various damper angles (60°, 75°, 90° and 120°) were chosen to fabricate the L2 dampers. A 90° damper angle was selected to for the L1 and L3 dampers. These combinations made the experimental program feasible and provided sufficient information to evaluate the contribution of various curved damper designs to structural performance enhancement.

By adjusting the damper lengths and damper angles, various eccentricities between the damper centroid and axis connecting the two damper ends could be achieved to identify the damper geometry influence on structural performance. The test frames were labelled according to the adopted damper geometry, as described in Table 2. For example, L2-75 indicated a semi-rigid frame equipped with curved dampers with damper length and damper angle equaling 537 mm and 75°, respectively.

### *3.3. Test set-up and loading process*

Each test frame was hinged to a stiffened floor beam at the column bottoms and attached to a servo-controlled hydraulic actuator, SCHENCK PGz1.0X with 1000kN capacity and 1000 mm stroke, supported by a reaction frame. A lateral support frame was adopted in the central portion of the test frame so that frame stability could be sustained during the loading process. The test set-up is shown in Fig. 8. Each test frame was subjected to cyclic loading, generated by a series of increasing displacement commands until 5% drift ratio was achieved, as shown in Fig. 9. Strain gauges and linear variable differential transducers (LVDTs) were installed on the beam, column and curved dampers to measure the structural responses for later comparisons and performance evaluation. The results obtained from the cyclic loading tests can also be used as data for comparisons should further evaluation of dynamic behavior of single or multi-story frames be desired.

## 4. Experimental results

### *4.1. Failure patterns*

Rigid frame failure was initiated by the flange yielding at the beam-to-column connections. Subsequent flange local buckling was observed when the test frame story drift was increased. For semi-rigid frames subjected to cyclic loading, yielding was first observed at the steel angles that connected the beam and columns. Cumulative plastic deformation leading to steel angle fracture was exhibited when the test frame drift ratio was increased.

The semi-rigid frames with curved damper failure patterns began with the yielding of curved dampers and followed with the yielding of steel angles at larger drift, as shown in Fig. 10. The figure shows that the maximum strain occurred at the inner-center position of the curved damper due to the combined effect of axial force and additional moment from damper eccentricity.

The damper yield zone progressed when frame deformation increased. Fig. 11 shows the yield regions of the six dampers used in the frame tests when they were subjected to 5% drift. The figure shows that the yield region magnitudes were approximately two thirds of the damper size, which justified the energy dissipation effectiveness of the proposed dampers. It is worth noting from the test observations that no damper plate buckling was exhibited during the loading process, as the device behavior was governed by the curved plate bending. This phenomenon validated the stability of the proposed damper under large deformation.

### *4.2. Deformation capacity*

The hysteretic loops for all test frames are shown in Fig. 12. Although stable hysteretic behavior was sustained when the test frame story drift reached 5%, the various achievable drifts at which

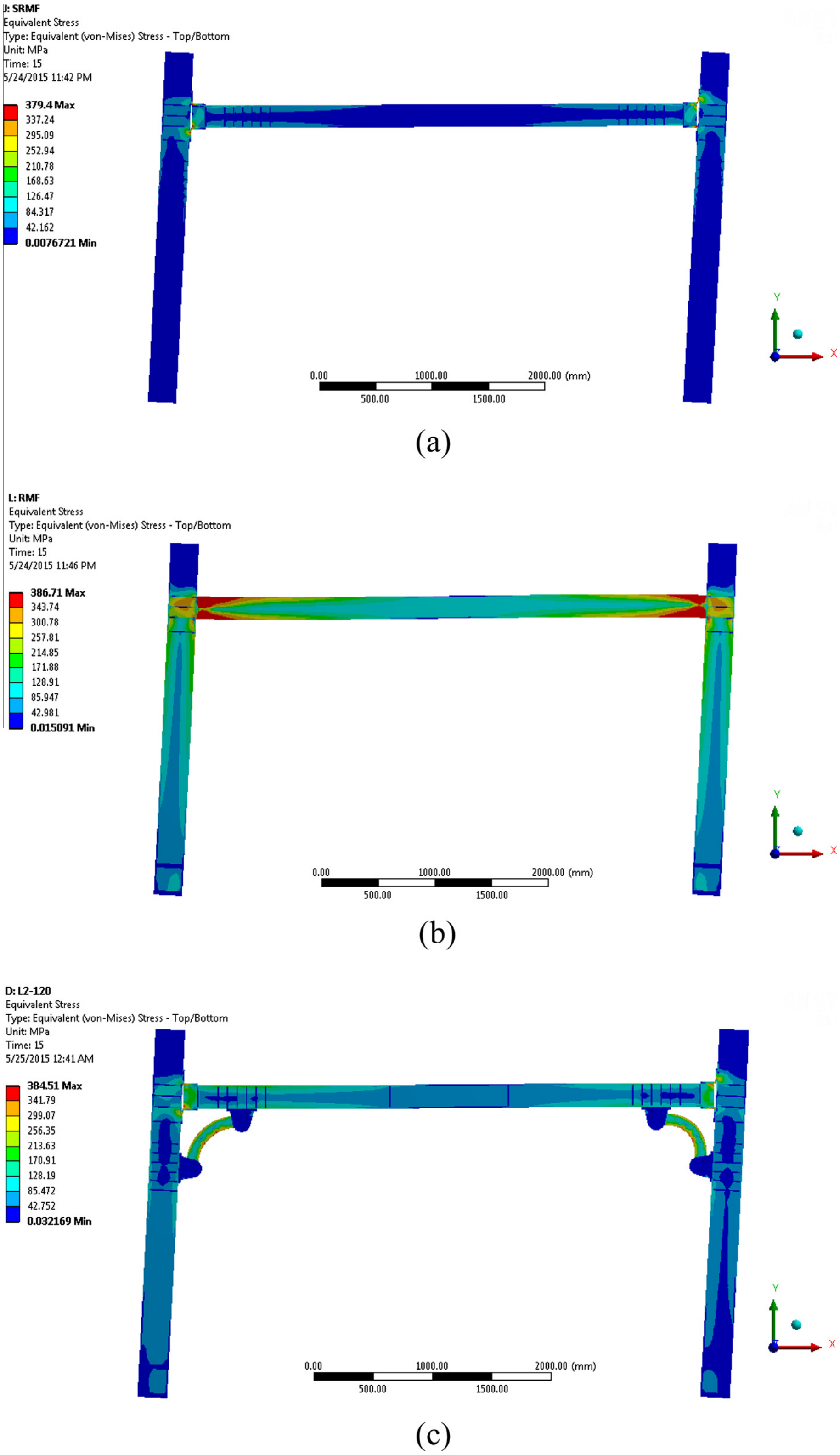

**Fig. 4.** Stress distribution of steel frames. (a) Semi-rigid frame; (b) rigid frame; (c) semi-rigid frame with curved dampers.

major structural members became inelastic distinguished the design deformational capacity. Observed from the tests, the semi-rigid frame (SRMF) showed no failure at the beams and columns, except for the top and seat angles in connections, when the structure was subjected to 5% drift. Limited and simple steel angle replacements in the connections greatly reduced the costs when structure rehabilitation was considered. For a rigid frame (RMF) subject to cyclic load, the beam reached yielding at 1% drift, followed by progressive plastic deformation accumulation in the member. Beam replacement after loading became inevitable

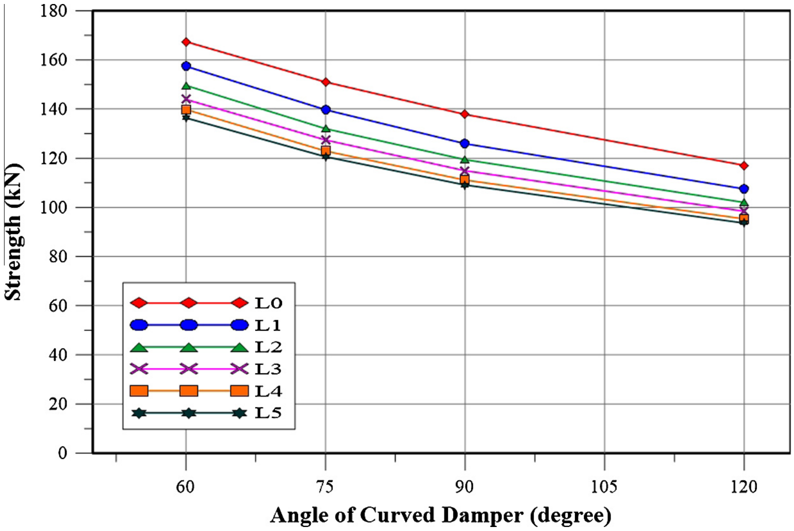

**Fig. 5.** Relationship between frame strength and damper geometries.

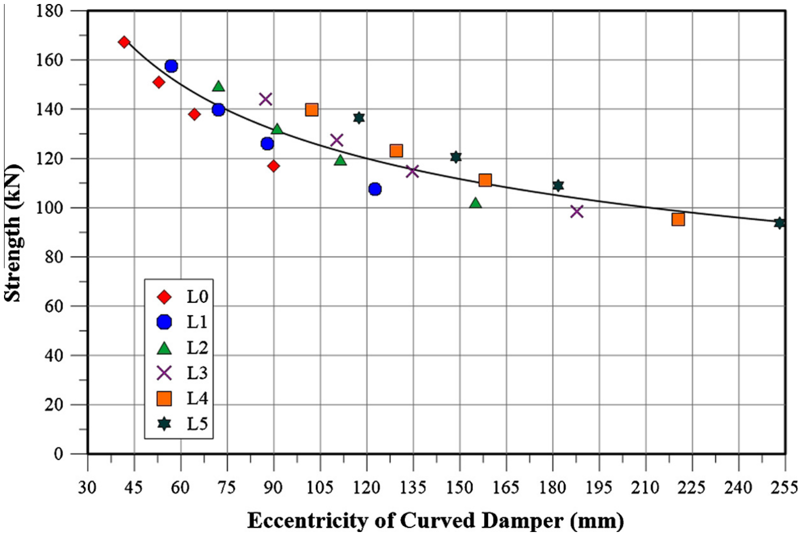

**Fig. 6.** Relationship between frame strength and damper eccentricities.

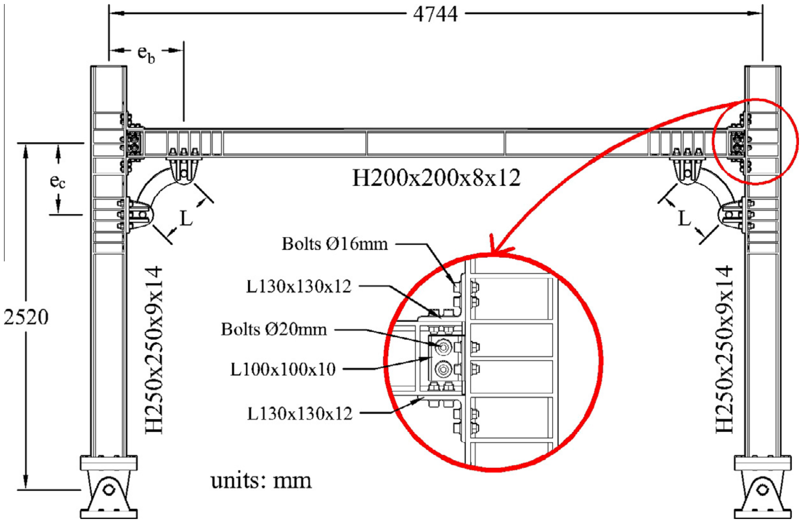

**Fig. 7.** Details of the test frames.

**Table 2**
Details of test frames.

| Frame label | Beam to column connection | $e_b$ (mm) | $e_c$ (mm) | $L$ (mm) |
|---|---|---|---|---|
| SRMF | Semi-rigid | N.A. | N.A. | N.A. |
| RMF | Rigid | N.A. | N.A. | N.A. |
| L1-90 | Semi-rigid | 765 | 765 | 424 |
| L2-60 | Semi-rigid | 845 | 845 | 537 |
| L2-75 | Semi-rigid | 845 | 845 | 537 |
| L2-90 | Semi-rigid | 845 | 845 | 537 |
| L2-120 | Semi-rigid | 845 | 845 | 537 |
| L3-90 | Semi-rigid | 925 | 925 | 651 |

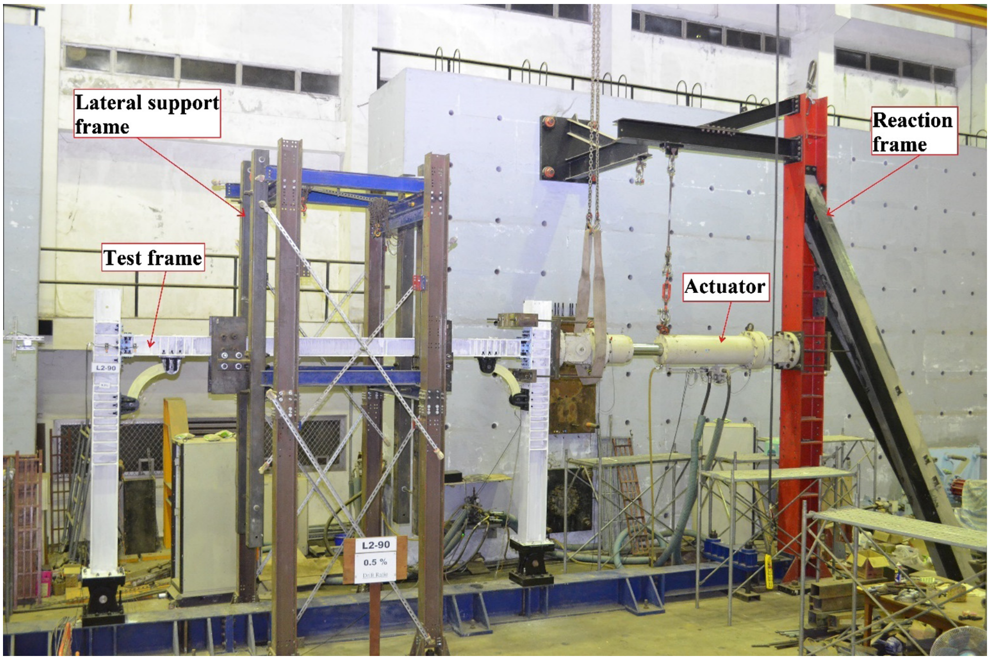

**Fig. 8.** Test set-up.

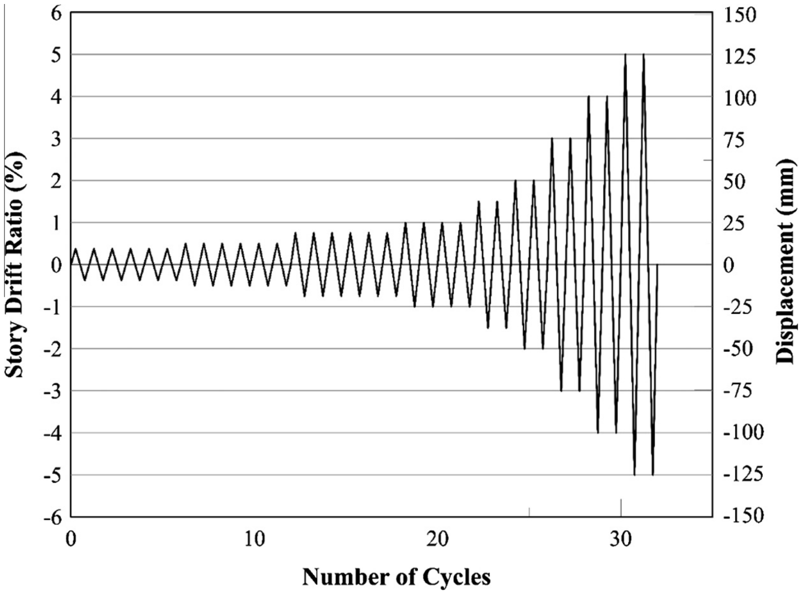

**Fig. 9.** Loading history.

making the use of rigid connections less desirable, if deformation capacity is a concern.

For semi-rigid frames with curved dampers, the deformation process was similar to that of the SRMF, except that the dampers

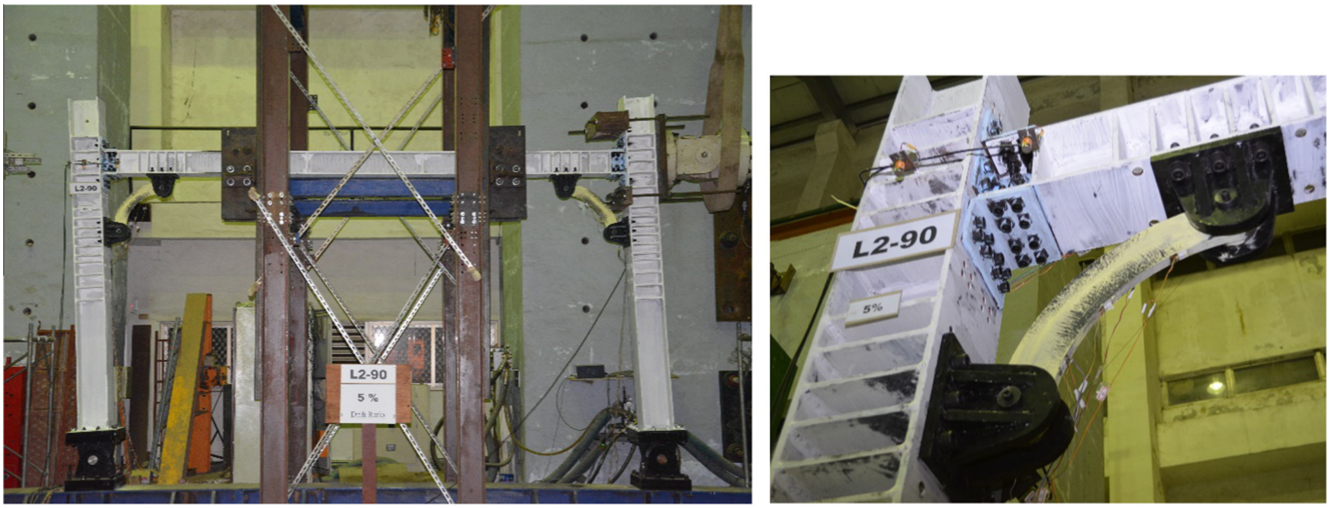

(a) (b)

**Fig. 10.** Failure patterns of semi-rigid frames with curved dampers. (a) Global view; (b) close-up view of curved damper.

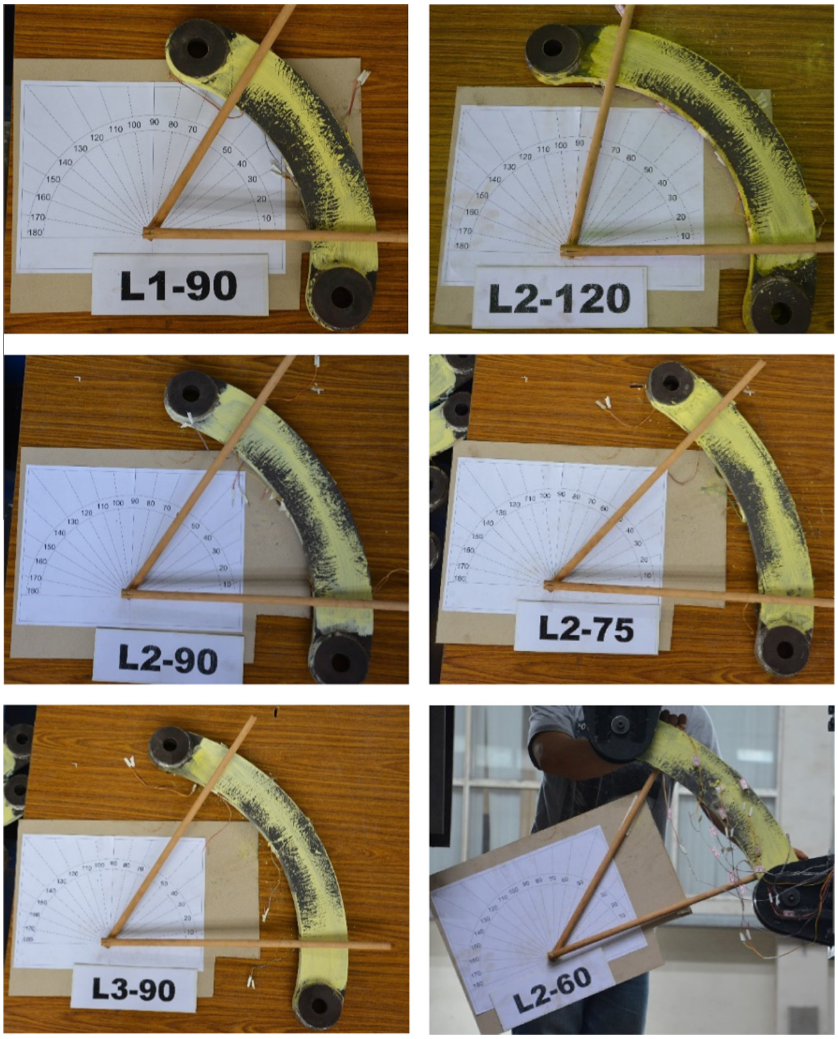

**Fig. 11.** Yield regions of dampers with various geometries.

reached yielding at various drifts prior to the steel angles, approximately at 0.5–0.75%. The curved dampers exhibited stable hysteretic behavior and provided continuous support to the frame structures after the devices became inelastic. The adequate load-resisting capability of the curved dampers effectively sustained the frame strength; prevented structural members from reaching

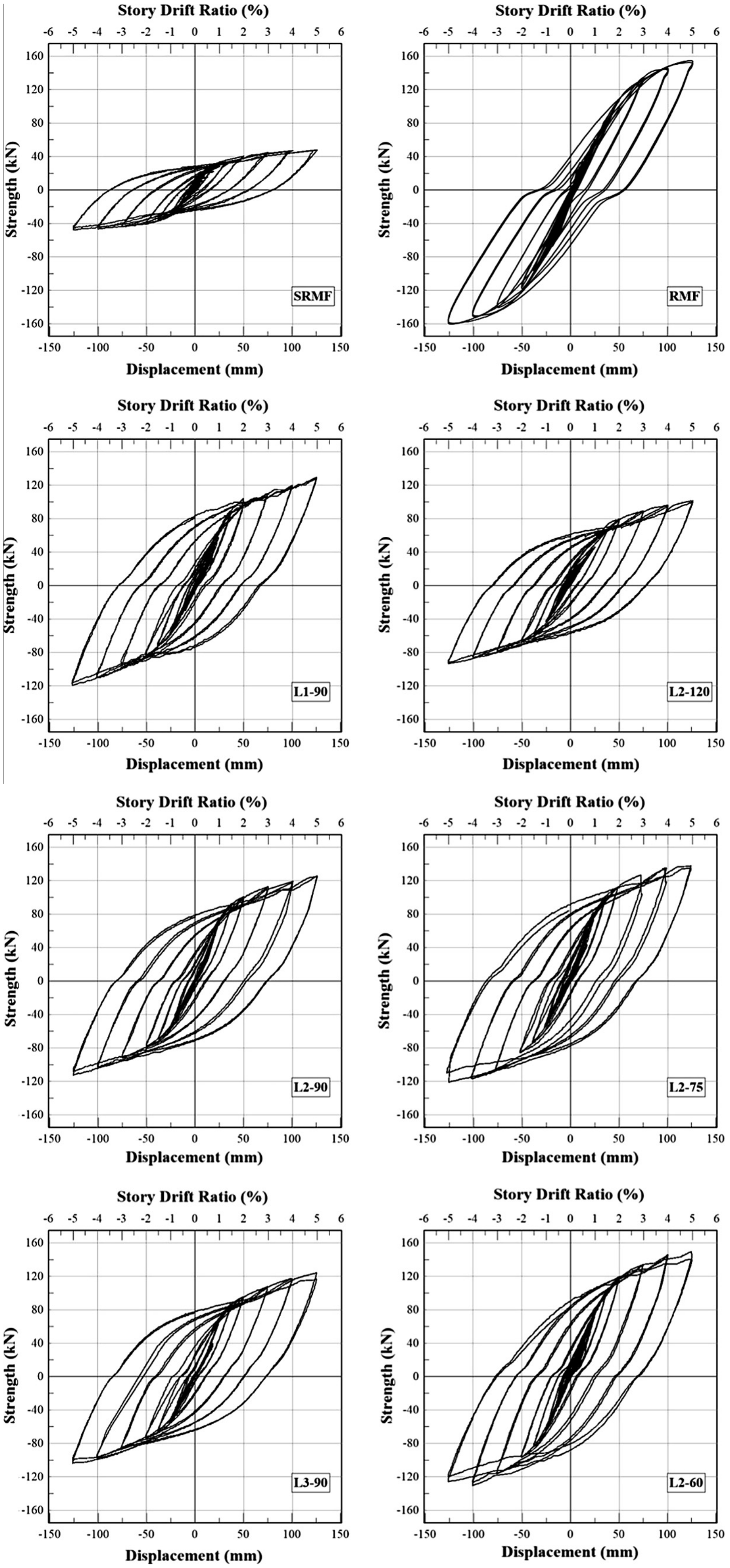

**Fig. 12.** Hysteretic loops for all test frames.

yielding at 5% drift, and thus greatly enhanced the structure performance.

### 4.3. Stiffness

Fig. 13 shows the normalized stiffness with respect to a semi-rigid frame for all test specimens. The figure shows that curved dampers effectively enhanced the structure stiffness. For example, the stiffness of semi-rigid frames with the proposed curved dampers was much higher than that for the semi-rigid moment frame, ranging from 1.29 to 2.36, and was higher than that for the rigid moment frame, when adequate curved dampers were adopted. Table 3 compares the elastic stiffness of all test specimens. The frame stiffness with curved dampers was adequately sustained after damper yielding, hence justifying the design method effectiveness. It should be noted from the comparisons that the stiffness of semi-rigid frames with steel curved dampers is slightly higher than that of the RMF system, which might shorten the vibration period of the system and cause higher seismic action. Therefore, a pinned connection between the beam and the column would be feasible when application of the proposed curved damper is considered.

The damper geometry effect on the structural stiffness can be described in separate groups. Fig. 13(a) shows that the stiffness gains in frame structures due to variations in damper length were similar. However, when curved dampers with various angles were adopted in the structures, significant differences in stiffness would be displayed, as shown in Fig. 13(b). This phenomenon could be attributed to the damper eccentricity magnitude, as larger damper angle would incur higher eccentricity and lower structural stiffness.

### 4.4. Strength

The strength of the test frames is listed in Table 4. The table shows that the semi-rigid moment frame (SRMF) strength was insufficient, approximately 31% that of the rigid moment frame (RMF). Significant strength enhancement was achieved when adequate curved dampers were installed in the semi-rigid frame. The strength gains ranged from 2.13 to 3.19 when compared with the SRMF strength. The highest strength, achieved in L2-60, was also equivalent to that of the rigid frame. These results validated the applicability of curved dampers in structural strength enhancement.

**Table 3**
Comparisons of normalized stiffness.

| Specimen | Elastic stiffness (kN/m) | Normalized stiffness with respect to SRMF | Normalized stiffness with respect to RMF |
|---|---|---|---|
| SRMF | 1481 | 1 | 0.62 |
| RMF | 2381 | 1.61 | 1 |
| L1-90 | 2804 | 1.89 | 1.18 |
| L2-60 | 3492 | 2.36 | 1.47 |
| L2-75 | 3280 | 2.21 | 1.38 |
| L2-90 | 2751 | 1.86 | 1.16 |
| L2-120 | 1905 | 1.29 | 0.8 |
| L3-90 | 2646 | 1.79 | 1.11 |

Damper length and damper angle effects on the strength improvements of frame structures can be explained by the results shown in Fig. 14. Fig. 14(a) shows that the variation in strength due to different damper lengths was not significant. However, for curved dampers with different angles, that is 120°, 90°, 75° and 60°, respectively; changing the angles would significantly influence the eccentricity magnitude therefore affecting the structural strength as well, as shown in Fig. 14(b).

### 4.5. Energy dissipation

Energy dissipation was evaluated by the cumulative hysteretic curve area of each test frame. Fig. 15 shows the cumulative energy dissipation for all specimens loaded to 5% story drift. The comparison shows that significant improvement in energy dissipation was achieved whenever the curved damper was adopted in the structural design. The normalized energy dissipation for all test frames with respect to SRMF and RMF, respectively, is listed in Table 5. The

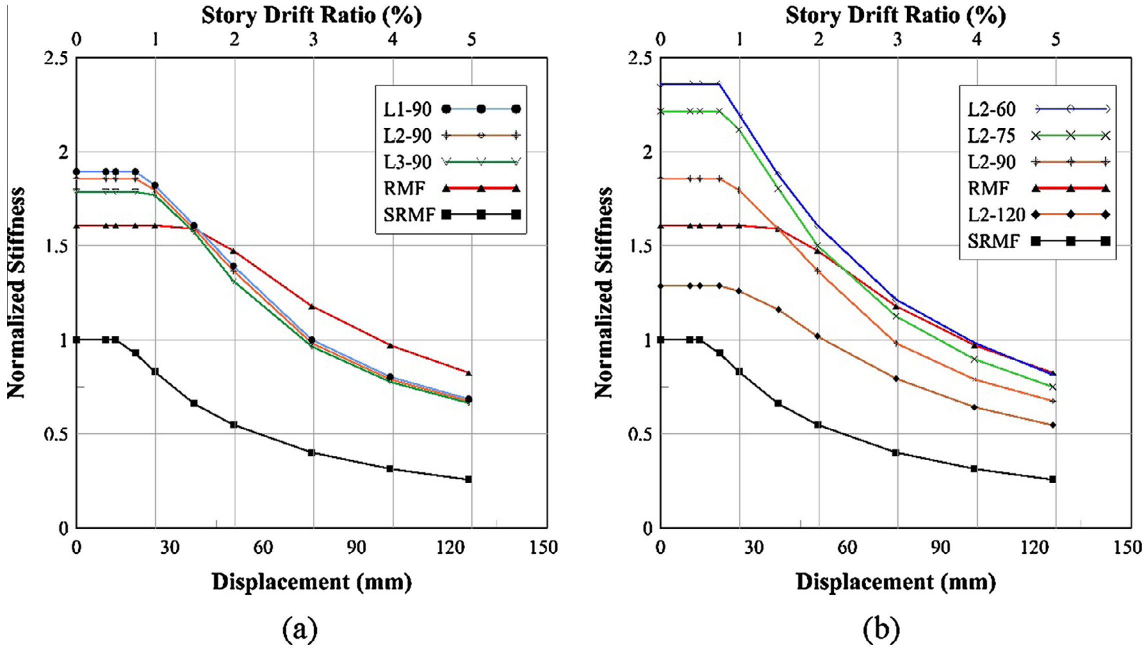

**Fig. 13.** Comparisons of normalized stiffness. (a) Dampers with the same angle, however different length; (b) dampers with the same length, however different angles.

**Table 4**
Comparisons of strength for the test frames.

| Specimen | Strength at 5% drift (kN) | Normalized strength with respect to SRMF | Normalized strength with respect to RMF |
|---|---|---|---|
| SRMF | 48 | 1 | 0.31 |
| RMF | 154 | 3.21 | 1 |
| L1-90 | 128 | 2.67 | 0.83 |
| L2-60 | 153 | 3.19 | 0.99 |
| L2-75 | 140 | 2.92 | 0.91 |
| L2-90 | 126 | 2.63 | 0.82 |
| L2-120 | 102 | 2.13 | 0.66 |
| L3-90 | 124 | 2.58 | 0.8 |

comparison shows that the energy dissipation gains for all semi-rigid frames with curved dampers were significant, ranging from 1.92 to 2.62, when compared with SRMF. The largest energy dissipation gain found in semi-rigid frame with curved damper, L2-60, was 2.62 times that of SRMF and 1.77 times that of the moment frame with more costly rigid connections, RMF. These characteristics validated the curved damper effectiveness in upgrading the seismic performance of steel frame designs.

The curved damper geometries, i.e. damper length and damper angle, effects on the structural performance are distinguished in Fig. 15(a) and (b). Fig. 15(a) shows that similar improvement in energy dissipation was exhibited in the test frames when curved dampers with different lengths with the same angle were adopted. Test frames with curved dampers with various angles showed significant variation in energy dissipation capability, as shown in Fig. 15(b). For example, L2-60 with the smallest angle showed the highest energy dissipation and L2-120 with the largest angle exhibited the lowest energy dissipation improvement. The test results showed that a decrease in damper angle would lead to energy dissipation improvement. These phenomena could be attributed to the strength of the adopted curved dampers because dampers with smaller angles incurred smaller eccentricity, exhibited higher damper strength and subsequently contributed more to the frame strength, hysteretic response and energy dissipation

## 5. Performance evaluation

For adequate seismic design, the structures should possess high strength, adequate deformation capacity and significant energy dissipation. To adequately evaluate the effectiveness of the proposed method in performance improvements, the above-mentioned criteria were considered simultaneously. Fig. 16 correlates the energy dissipation and frame strength for all test frames. It was found from the comparisons that the strength and energy dissipation of test frames with curved dampers, regardless of the damper dimensions, were simultaneously enhanced when compared with the semi-rigid frame. Further test result comparisons revealed that the damper angles played more important roles than the damper lengths in affecting the structural performance. Among these frames, the highest gains in strength and energy dissipation were achieved with L2-60.

The performance of L2-60, including deformation capacity, stiffness, strength and energy dissipation, was further compared with those of the rigid frame, as shown in Fig. 17. The figure shows that performance superior to the rigid frames could be achieved in semi-rigid frames when adequate curved dampers were adopted. These characteristics validated the applicability of the proposed damper in engineering practice.

The efficiency of the proposed curved dampers can be further validated by comparing the performance of the devices with those of frames strengthened with buckling restrained braces (BRB) [34], and frames strengthened with triangular-plate added damping and stiffness (TADAS) devices [35]. For example, the strength gains for semi-rigid frames with various curved dampers ranged from 2.13 to 3.19, which are compatible with the gains achieved in the above-mentioned frames with BRB and TADAS, 2.2 and 2.1, respectively. Effectiveness of curved dampers can be further validated by the variation in structural deformation capacity. For frames with curved dampers, the achievable drift ratio was the same as that of frame without damper. However, for frames with BRB and TADAS, the achievable deformation capacity was reduced to 60% and 45% of the original deformation capability, respectively. Simultaneous improvements in strength and deformation capacity effec-

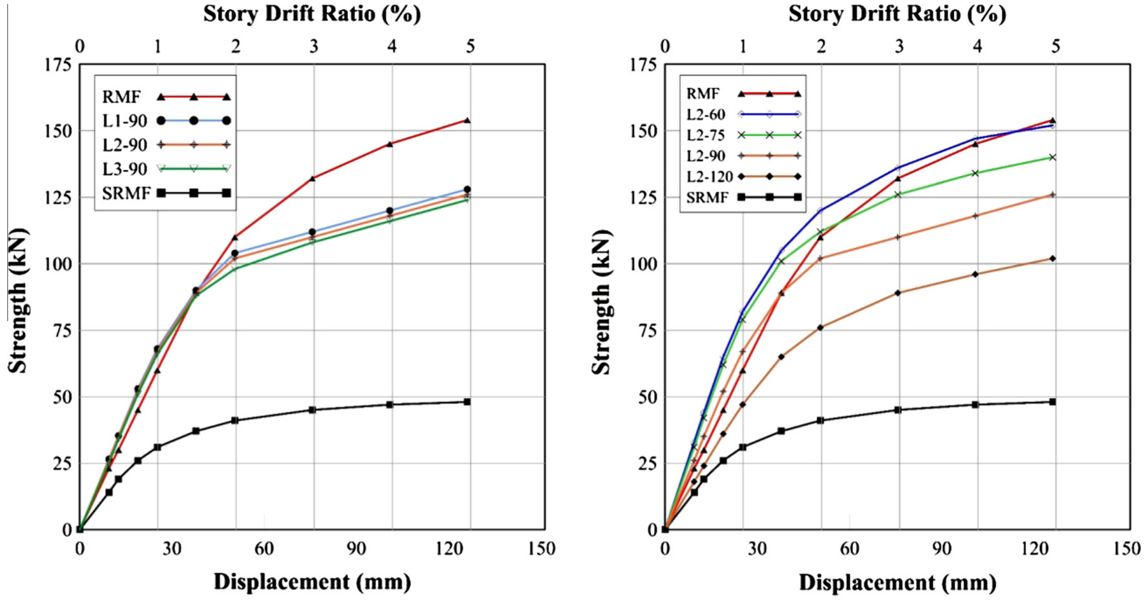

(a) (b)

**Fig. 14.** Comparisons of strength. (a) Dampers with the same angle, however different length; (b) dampers with the same length, however different angles.

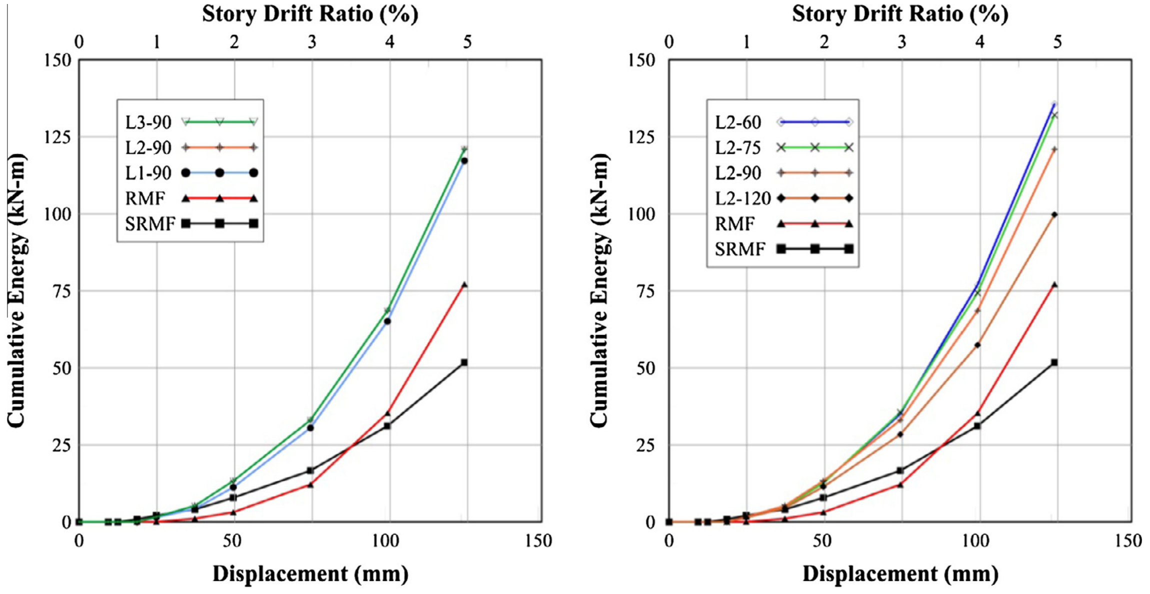

(a) (b)

**Fig. 15.** Comparisons of energy dissipation. (a) Dampers with the same angle, however different length; (b) dampers with the same length, however different angles.

**Table 5**
Comparisons of energy dissipation for the test frames.

| Specimen | Energy dissipation (kN-m) | Normalized energy dissipation with respect to SRMF | Normalized energy dissipation with respect to RMF |
|---|---|---|---|
| SRMF | 52 | 1 | 0.68 |
| RMF | 77 | 1.48 | 1 |
| L1-90 | 117 | 2.25 | 1.52 |
| L2-60 | 136 | 2.62 | 1.77 |
| L2-75 | 132 | 2.54 | 1.71 |
| L2-90 | 121 | 2.33 | 1.57 |
| L2-120 | 100 | 1.92 | 1.30 |
| L3-90 | 115 | 2.21 | 1.49 |

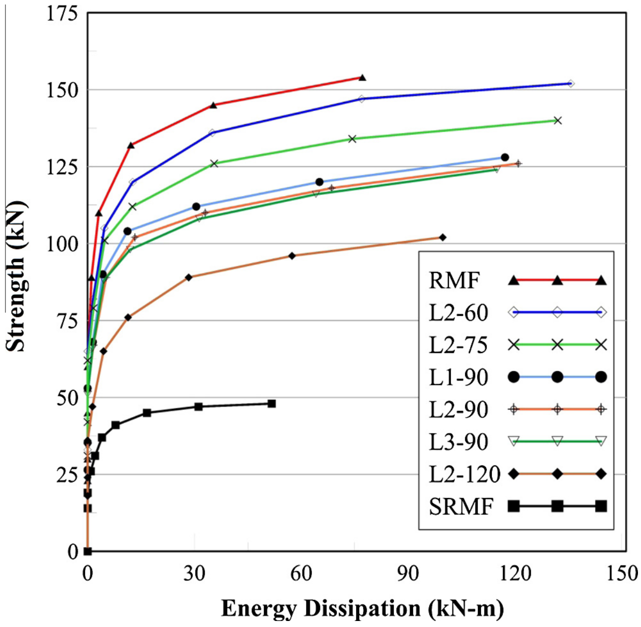

**Fig. 16.** Correlation between energy dissipation and strength for all test frames.

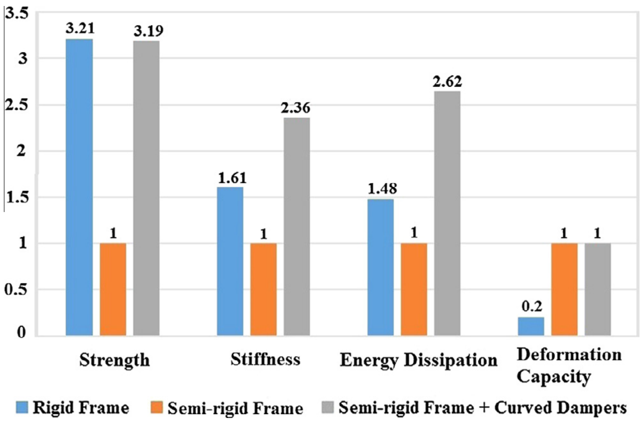

**Fig. 17.** Comparison of performance among rigid frame, semi-rigid frame and L2-60.

tively justified the feasibility of the proposed curved damper in the engineering designs.

## 6. Conclusions

This study focused on the performance improvement of framed structures with proposed steel curved dampers. A series of cyclic load tests were conducted on the semi-rigid frame, rigid frame and semi-rigid frames with various curved damper placements. It was found from the tests that the curved dampers exhibited stable hysteretic behavior under compression and tension, and thus are suitable devices for seismic strengthening or retrofit of structures.

Further comparisons on the test results showed that significant improvements in strength, stiffness and energy dissipation were achieved when the proposed curved dampers were added to the semi-rigid frames. The highest gains achieved in L2-60 were 3.19 times in strength, 2.36 times in stiffness and 2.62 times in energy dissipation, respectively, when compared with those of a semi-rigid moment frame. These performances were also superior to those of the rigid frame which validated the effectiveness of the proposed damper design in frame structure performance improvement. It should be noted that information obtained from this preliminary investigation constructed the data for comparisons. Subsequent study on the dynamic behavior of multi-story framed structures is in process to further validate the feasibility of the proposed design method.

## Acknowledgments

The test specimens were partially supported by the National Center for Earthquake Engineering Research, Taiwan, which is gratefully acknowledged.

## References

[1] Kim J, Park J. Design of steel moment frames considering progressive collapse. Steel Compos Struct 2008;8:85–98.

[2] Hsu HL, Li ZC. Seismic performance of steel frames with controlled buckling mechanisms in knee braces. J Constr Steel Res 2015;107:50–60.

[3] Lee CH, Kim JH. Seismic design of reduced beam section steel moment connections with bolted web attachment. J Constr Steel Res 2007;63:522–31.

[4] Palermo M, Ricci I, Gagliardi S, Silvestri S, Trombetti T, Gasparini G. Multi-performance seismic design through an enhanced first-storey isolation system. Eng Struct 2014;59:495–506.

[5] Palermo M, Silvestri S, Gasparini G, Trombetti T. Crescent shaped braces for the seismic design of building structures. Mater Struct 2015;48:1485–502.

[6] Rai DC, Annam PK, Pradhan T. Seismic testing of steel braced frames with aluminum shear yielding dampers. Eng Struct 2013;46:737–47.

[7] Samani HR, Mirtaheri M, Zandi AP. Experimental and numerical study of a new adjustable frictional damper. J Constr Steel Res 2015;112:354–62.

[8] Wongpakdee N, Leelataviwat S, Goel SC, Liao WC. Performance-based design and collapse evaluation of buckling restrained knee braced truss moment frames. Eng Struct 2014;60:23–31.

[9] Abdalla KM, Abu-Farsakh GAR, Barakat SA. Experimental investigation of force-distribution in high-strength bolts in extended end-plate connections. Steel Compos Struct 2007;7:87–103.

[10] Coelho AMG, Bijlaard FSK. Experimental behavior of high strength steel end-plate connections. J Constr Steel Res 2007;63:1228–40.

[11] Dubina D, Stratan A. Behaviour of welded connections of moment resisting frames beam-to-column joints. Eng Struct 2002;24:1431–40.

[12] Moncarz DP, McDonald BM, Caligiuri RD. Earthquake failures of welded building connections. Int J Solids Struct 2001;38:2025–32.

[13] Oh SH, Kim YJ, Ryu HS. Seismic performance of steel structures with slit dampers. Eng Struct 2009;31:1997–2008.

[14] Ramirez CM, Lignos DG, Miranda E, Kolios D. Fragility functions for pre-Northridge welded steel moment-resisting beam-to-column connections. Eng Struct 2012;45:574–84.

[15] Silwal B, Michael RJ, Ozbulut OE. A superelastic viscous damper for enhanced seismic performance of steel moment frames. Eng Struct 2015;105:152–64.

[16] Abolmaali A, Kukreti A, Motahari A, Ghassemieh M. Energy dissipation characteristics of semi-rigid connections. J Constr Steel Res 2009;65:1187–97.

[17] Gerami M, Saberi H, Saberi V, Daryan AS. Cyclic behavior of bolted connections with different arrangement of bolts. J Constr Steel Res 2011;67:690–705.

[18] Gong Y. Ultimate tensile deformation and strength capacities of bolted-angle connections. J Constr Steel Res 2014;100:50–9.

[19] Lee SS, Moon TS. Moment-rotation model of semi-rigid connections with angles. Eng Struct 2002;24:227–37.

[20] Lin XC, Okazaki T, Nakashima M. Bolted beam-to-column connections for built-up columns constructed of H-SA700 steel. J Constr Steel Res 2014;101:469–81.

[21] Pucinotti R. Cyclic mechanical model of semi-rigid top and seat and double web angle connections. Steel Compos Struct 2006;6:139–57.

[22] Vu AQ, Leon RT. Vibration analysis of steel frames with semi-rigid connections on an elastic foundation. Steel Compos Struct 2008;8:265–80.

[23] Yang B, Tan KH. Robustness of bolted-angle connections against progressive collapse: mechanical modelling of bolted-angle connections under tension. Eng Struct 2013;57:153–68.

[24] Chou CC, Tsai KC, Wang YY, Jao CK. Seismic rehabilitation performance of steel side plate moment connections. Earthq Eng Struct Dyn 2010;39:23–44.

[25] Ciutina AL, Dubina D. Seismic behaviour of steel beam-to-column joints with column web stiffening. Steel Compos Struct 2006;6:493–512.

[26] Climent AB. A brace-type seismic damper based on yielding the walls of hollow structural sections. Eng Struct 2010;32:1113–22.

[27] Kang JD, Tagawa H. Seismic performance of steel structures with seesaw energy dissipation system using fluid viscous dampers. Eng Struct 2013;56:431–42.

[28] Kim T, Whittaker AS, Gilani ASJ, Bertero VV, Takhirov SM. Cover-plate and flange-plate steel moment-resisting connections. J Struct Eng-ASCE 2002;128. 484-82.

[29] Lee CH, Jeon SW, Kim JH, Uang CM. Effects of panel zone strength and beam web connection method on seismic performance of reduced beam section steel moment connections. J Struct Eng ASCE 2005;131:1854–65.

[30] Lehman DE, Roeder CW, Herman D, Johnson S, Kotulka B. Improved seismic performance of gusset plate connections. J Struct Eng ASCE 2008;134:890–901.

[31] Piedrafita D, Cahis X, Simon E, Comas J. A new modular buckling restrained brace for seismic resistant buildings. Eng Struct 2013;56:1967–75.

[32] Yoo JH, Lehman DE, Roeder CW. Influence of connection design parameters on the seismic performance of braced frames. J Constr Steel Res 2008;64:607–23.

[33] ANSYS. Workbench user's guide. ANSYS Inc.; 2013.

[34] Jia M, Lu D, Guo L, Sun L. Experimental research and cyclic behavior of buckling-restrained braced composite frame. J Constr Steel Res 2014;95:90–105.

[35] Saeedi F, Shabakhty N, Mousavi SR. Seismic assessment of steel frames with triangular-plate added damping and stiffness devices. J Constr Steel Res 2016;125:15–105.